1. Introduction

Small punch tests (SPTs) have been successfully employed for decades for the mechanical characterization of different metallic [1-6] and non-metallic materials [7,8]. One of the advantages of this test lies in the very small size of the specimens employed, with a characteristic length (side or diameter) smaller than 10 mm and thickness of 0.5 mm or lower. These specimens are firmly clamped between two circular dies and are bi-axially deformed into a circular hole until failure by means of an hemispherical punch, as displayed in Figure 1.

The "load-punch displacement" record obtained from the test can be used to estimate several "conventional" mechanical parameters [5,9]. Figure 2 shows a typical load-displacement response obtained with a ductile steel specimen, identifying different zones (I to IV), where several points of the curve, relevant to tensile parameter correlation, are highlighted. The initial slope of the curve could be related to the elastic modulus [3]; the P_y load, located in the transition between the elastic (I) and the plastic (II) zones, related to the yield stress, σ_y [5,9]; the maximum load, P_m, related to the ultimate tensile strength, σ_u [5,9]; the maximum displacement, d_m, related to the tensile elongation, $e(\%)$ [10,11]; and the area under the load-displacement curve, W_u, related to the fracture toughness [9,12]. Some of the typical relationships between the aforementioned SPT parameters and the tensile properties are:

$$\sigma_y = \alpha \frac{P_y}{t^2} \quad (1)$$

$$\sigma_u = \beta \frac{P_m}{t^2} \quad (2)$$

$$e(\%) = \gamma \frac{d_m}{t} \quad (3)$$

being t the initial specimen thickness and α, β and γ the characteristic material coefficients.

To a much lesser extent, the SPT has also been employed in the characterization of polymeric materials [13-19]. Most of the studies on these materials have been purely devoted to analyze the form of the SPT curves [13,15], and correlations between the tensile properties of polymers and their corresponding SPT parameters are yet to be identified. Therefore, it seems to be particularly appealing to investigate whether or not it is possible to derive any correlation between the SPT parameters and those commonly employed to characterize their mechanical properties.

In a recent study [16] using polylactide acid (PLA) modified with montmorillonite as specimens, the relationship between the yield strength and the P_{ym}/t^2 SPT parameter was established (being P_{ym} the load corresponding to the first maximum obtained in the SPT record). In this same study, the area under the SPT curve was also related to the essential work of fracture.

More recently, Maspoch et al. [17] have also investigated the modification of the ductile-to-brittle transition of the PLA related to the time elapsed after the application of a de-aged thermal treatment by means of the SPT. They also established a correlation between the slope of the SPT curve (defined in the zone just before the first local maximum of the curve) divided by the specimen thickness (Slope/t) and the tensile elastic modulus.

All these correlations were corroborated in a further study [18] using other type of polymers. Good correlations were obtained between the elastic modulus and yield strength with the respective SPT

parameters, Slope/t and P_{ym}/t^2, but the corresponding relations were markedly different than the ones obtained [17], so that a systematic experimental program is still necessary to ensure the applicability of the SPT to the mechanical characterization of polymers.

Consequently, the objective of this paper is to analyze whether the SPT is a useful tool for the assessment of the most characteristic tensile mechanical properties or not. A possible correlation with those results from standard tensile specimens is also discussed.

2. Materials

Four different types of polymers commonly used as films and laminates were studied in this work, namely polypropylene (PP), polyethylene terephthalate (PET), poly (lactic acid) and ethylene vinyl alcohol (EVOH). The aim was to study the influence of the molecular structure and morphology on the SPT properties. There- fore, two amorphous (PET and PLA) as well as two semicrystalline materials (PP and EVOH) were selected. Moreover, the effect of the dispersion state of a nanofiller (montmorillonite, MMT) on an amorphous (PLA) and on a semicrystalline polymer (EVOH) was assessed. This type of nanofiller is incorporated into polymers in order to improve certain properties, e.g. in the case of PLA and EVOH it is well known that the barrier properties improve upon MMT incorporation which is beneficial for food packaging.

Injected PP, which had been used in [19] to study the effect on mechanical strength of adding different percentages of recycled material, corresponded to grade BASELL X9077. PET and PETg were supplied by NUDEC in form of extrusion-calendered laminates. For the synthesis of PETg, CHDM is used to introduce discontinuities in the polymer chain in order to make the crystallization process more difficult, this material being nearly amorphous even in the form of thick plates.

PLA 2002D (96% L-lactide isomer) was supplied by NatureWorks and a commercial EVOH (Soarnol®AT44 03B) containing 44% mol of ethylene was used. Organically modified montmorillonite (Cloisite 30B), with 30 wt.% organic modifier, was supplied by Southern Clay Products.

Neat PLA (PLA_0%) and EVOH (EVOH_0%) laminates as well as their nanocomposites were prepared by twin screw extrusion in the *Centre Català del Plàstic.* Nanocomposites with different MMT concentrations were prepared in a three-step melt-extrusion process using a Collin ZK-35 co-rotating twin-screw extruder (L/D = 36; D = 25 mm). The first step consisted in the preparation of a masterbatch containing 10 wt% of clay. In the second step this masterbatch was reprocessed in order to achieve a homogeneous mixture. In a third step the masterbatch was diluted with the polymer matrix to the desired concentrations. In all stages, the twin- screw rotation speed was set at 80 rpm. In the case of EVOH the temperatures were between 160 ºC in the feed section and 220 ºC at the extrusion die and in the case of PLA the temperatures were between 150 and 175 º C. EVOH was prepared with nominal clay content of 1 (EVOH_1%) and 2.5 (EVOH_2.5%) wt% and PLA contained 0.5 (PLA_0.5%) and 2.5 (PLA_2.5%) wt% of MMT. Sample preparation is described in detail in Refs. [20,21].

Films of PLA were subjected to a de-aging thermal treatment [16], consisting of heating to 60 º C for 20 min and quenching by immersion in an ice-water bath for 5 min. These

samples were coded with a T in order to indicate the thermal treatment (PLA_0T, PLA_0.5T and PLA_2.5T).

3. Tensile and small punch tests

The mechanical characterization of the different polymers was carried out using tensile and SPT tests. While some experiments were conducted in different laboratories, special care is taken to ensure that the same conditions apply in all case studies. In the case of polypropylene, analyzed at the University of Burgos, 5A type standard tensile specimens and rectangular samples (60 x 10 x 4 mm), both obtained by an injection process, were supplied by the manufacturer [19]. The rest of the polymers were manufactured in the Centre Catalá del Plastic. In these cases, the tensile specimens had a standard type IV geometry and were extracted along the longitudinal direction of the films. Nominal SPT specimens with the thickness of the film were also machined.

All the mechanical tests were performed at room temperature. Tensile experiments were carried out according to the ASTM D-638 standard, under a crosshead rate of 10 mm/min, using a testing machine (5 kN load cell) and a video-extensometer to measure the specimen elongation. SPTs were conducted using the experimental device depicted in Figure 1, which was mounted on a universal testing machine. A punch with a diameter of 2.4 mm, a lower die with a diameter of 4 mm (with 0.5 mm corner radius), a CTOD extensometer for precise displacement determination and a punch drop rate of 0.5 mm/min were used in all cases. The thickness of the SPT specimens was obtained as the average of five measurements by means of a precision micrometer. A minimum of ten samples were used to characterize each material.

Figure 3 shows the most representative engineering tensile curves (Figure 3a) and the corresponding SPT load-displacement curves (Figure 3b) of PP, PET and PETg polymers.
The mechanical behavior of these three polymers is markedly different in terms of stress (load) and strain (displacement). Polypropylene is the polymer with the lowest strength at yield and also at final rupture, showing a tensile elongation less than 40%. PET has a high tensile strength but a very low strain at failure, as it fails in a brittle manner before general yielding. On the other hand, PETg has a slightly lower yield strength, but it then suffers necking and hardening, giving rise to an ultimate tensile strength similar to the yield strength but under a tensile elongation at failure of 160%.

Moreover, the SPT load-displacement curves of the three polymers (Figure 3b) are quite different. Polypropylene gives rise to the lowest strength but, under biaxial stress state, the displacement at failure of the three polymers is nearly equivalent. Analyzing the shape of the load-displacement curves, it is worth noting that the PP curve attains a maximum, which can be considered related to the material yield strength, with the load continuously decreasing afterwards until complete failure of the specimen. In the case of PET, the curve also has a maximum (P_{ym}), after which the specimen experiments necking and hardening until its final rupture. Finally, the PETg curve does not show the maximum seen in the other two, although an inflection point followed by a slight increase in the specimen stiffness can be observed in this same region (yield strength, P_{ym}).

Figure 4 represents the results obtained in the tensile and SPT tests with plain PLA specimens. Figure 4a shows the tensile behavior of a plain PLA (unreinforced) before and after applying the de-aging treatment. The main effect of this treatment consists of an important increase of tensile elongation (from 15% to 450%), along with minor decreases in strength and stiffness. On the other

hand, although it is not observed in the aforementioned figure, nanoclay additions affect the tensile properties of the PLA to a much lower degree [16].

The SPT curves of the PLA specimens (Figure 4b) resemble the tensile curves, giving rise to similar load trends, but lower displacement differences between PLA specimens. Moreover, as it was already observed with the other polymers, the one with the lowest ductility (PLA_0%) shows a clear yield zone (around the maximum in the SPT curve), while the material with the largest tensile elongation only shows an inflection point in the yield zone and a strong hardening afterwards.

Figure 5 gathers together the tensile and SPT curves of the EVOH polymers with different reinforcement levels. Under tensile loads, nanoclay reinforced EVOH polymers have lower strength and larger elongation than the unreinforced polymer (Figure 5a). Another feature previously observed on these films is the different mechanical behavior of samples machined from the sides of the film (EVOH_L) or from the center (EVOH_C), with these differences diminishing as nanoclay reinforcement increases [18].

When these polymers are tested by means of the SPT (Figure 5b), the resulting behavior is not very different to that observed under tensile loading. The unreinforced EVOH has greater stiffness and strength than the nanoclay reinforced grades. Differences between specimens machined from the center and sides of the films are also appreciated in the SPT's [18]. Again, it was observed that clear hardening after yielding in the tensile tests gives rise to SPT curves without a load maximum around the yield zone, but only one inflection point can be seen in these cases before the start of the hardening zone.

4. Characteristic parameters and correlations

Based on the analysis summarized before, along with results obtained by other researchers using polymers and knowledge derived from the application of SPT's to characterize metallic materials, appropriate values of loads and displacements associated to characteristic points of the SPT records have been defined. Figure 6 shows the most important points.

Firstly, the slope of the initial region of the SPT curve can be derived, mainly the elastic zone ($Slope_{ini}$). This value divided by the specimen thickness t was seen to be related to the tensile elastic modulus, E.

Secondly, the first maximum in the load-displacement SPT curve defines the yield point (P_{ym}, d_{ym}). This load divided by t^2 and this displacement divided by t should be related to the strength and strain at yield under tension (σ_y, ε_y). When a maximum in the SPT curve is not appreciated, but rather an inflection point, yield parameters can be obtained at this point, as shown in Figure 6.

In the case of metallic materials, there is also a clear relationship between the load and the displacement at failure in the SPTs and the ultimate tensile strength and tensile elongation. However, such correlations were not observed with polymers, as hardening and necking phenomena are clearly different under uniaxial and under biaxial stresses.

Figures 7, 8 and 9 show the regressions obtained with the polymers analyzed in this paper between the different SPT parameters and their corresponding tensile properties. Although certain dispersion was always obtained, the regressions are quite good.

Figure 7 reflects a good correlation between the tensile elastic modulus and the initial slope of the SPT curve, which was divided by the specimen thickness to obtain the same dimensions (MPa). In the case of metals, it is more difficult to derive the tensile elastic modulus from the SPT record, undoubtedly due to their much greater stiffness.

In the case of yield strength, the coefficient of determination obtained between this tensile property and the corresponding SPT parameter was high (R^2=0.9058).

On the contrary, the correlation obtained between the tensile yield strain and the d_{ym}/t parameter was very poor, although both varied in a similar trend. In this respect, the relatively small difference among ε_y of the analyzed polymers (between 2% and 4%) may play an important role.

5. Conclusions

The use of small punch Test in the mechanical characterization of different types of polymers has been thoroughly evaluated.

Under the biaxial stress state characteristic of SPTs, polymers generally behave in a more ductile manner than under uniaxial load, developing larger elongations at failure.

Yield region of a polymer can be easily identified in the Small Punch tests by a relative maximum in the load-displacement curve once exceeded the initial elastic region. That relative maximum is very clear in all polymers that show no hardening after yielding in the tension test, while those that harden after tensile yielding show one inflection point in the SPT record.
Unique and confident relationships between elastic modulus and yield strength tensile properties and characteristic SPT parameters were identified. Similar relationships could not be obtained in the case of the yield strain and strength and elongation at failure.

The SPT can be viewed as a useful tool for the mechanical characterization of polymers, as it only requires a very small specimen to easily and quickly obtain approximate values of the most characteristic tensile mechanical properties.

6. Ackowlegements

Authors gratefully acknowledge financial support of the Ministry of Economy and Competitiveness of Spanish, through grant MAT2014-58738-C3-1-R and MAT2013-40730-P.

References

[1] M.P. Manahan, A.S. Argon, O.K. Harling, The development of a miniaturized disk bend test for the determination of post irradiation mechanical properties, J. Nucl. Mater. 104 (1981) 1545–1550.
[2] X. Mao, H. Takahashi, Development of a further-miniaturized specimen of 3 mm diameter for tem disk (ø 3 mm) small punch tests, J. Nucl. Mater. 150 (1987) 42–52.
[3] V. Vorliceck, L.F. Exworthy, P.E.J. Flewitt, Evaluation of a miniaturized disc test for

establishing the mechanical properties of low alloy steels, J. Mater. Sci. 30 (1995) 2936–2943.
[4] E. Fleury, J.S. Ha, Small punch tests to estimate the mechanical properties of steels for steam power plant, Int. J. Pres. Ves. Pip. 75 (1998) 699–706.
[5] T.E. García, C. Rodríguez, F.J. Belzunce, C. Suárez, Development of a methodology to study the hydrogen embrittlement of steels by means of the small punch test, J. Alloy. Compd. 582 (2014) 708–717.
[6] E. Martínez-Pañeda, T.E. García, C. Rodríguez, Fracture toughness characterization through notched small punch test specimens, Mater. Sci. Eng., A 657 (2016) 422–430.
[7] S. Rasche, S. Strobl, M. Kuna, R. Bermejo, T. Lube, Determination of strength and fracture toughness of small ceramic discs using the small punch test and the ball-on-three-balls test, Proc. Mater. Sci. 3 (2014) 961–966.
[8] S. Soltysiak, M. Abendroth, M. Kuna, Y. Klemm, H. Biermann, Strength of _ne grained carbon-bonded alumina (Al2O3-C) materials, Ceram. Int. 40 (7A) (2014) 9555–9561.
[9] CEN Workshop Agreement, CWA 15627:2006 E. Small Punch Test Method for Metallic Materials, 2006.
[10] C. Rodríguez, J. García Cabezas, E. Cárdenas, F.J. Belzunce, C. Betegón, Mechanical properties characterization of heat affected zones using the small punch test, Weld. J. 88 (2009) 188s–192s.
[11] M. Fernández, C. Rodríguez, F.J. Belzunce, T.E. García, Use of small punch test to estimate the mechanical properties of powder metallurgy products employed in the automotive industry, Powder Metall. 58 (3) (2015) 171–177.
[12] J.H. Bulloch, Toughness losses in low alloy steels at high temperatures: an appraisal of certain factors concerning the small punch test, Int. J. Pres. Ves. Pip. 75 (1998) 791–804.
[13] S.M. Kurtz, J.R. Foulds, C.W. Jewett, S. Srivastav, A.A. Edidin, Validation of a small punch testing technique to characterize the mechanical behaviour of ultra-highmolecular-weight polyethylene, Biomaterials 18 (1997) 1659–1663.
[14] V.L. Giddings, S.M. Kurtz, C.W. Jewett, J.R. Foulds, A.A. Edidin, A small punch test technique for characterizing the elastic modulus and fracture behavior of PMMA bone cement used in total joint replacement, Biomaterials 22 (2001) 1875–1881.
[15] T.D.J. Jaekel, D.W. MacDonald, S.M. Kurtz, Characterization of PEEK biomaterials using the small punch test, J. Mech. Behav. Biomed. 4–7 (2011) 1275–1282.
[16] C. Rodríguez, F.J. Belzunce, D. Arencón, M.L.L. Maspoch, Small punch test on the analysis of fracture behaviour of PLA-nanocomposite, Polym. Test. 33 (2014) 21–29.
[17] M.L.L. Maspoch, O.O. Santana, J. Cailloux, E. Franco-Urquiza, C. Rodríguez, J. Belzunce, A.B. Martínez, Ductile-brittle transition behaviour of PLA/o-MMT films during the physical aging process, eXPRESS Polym. Lett. 9 (3) (2015) 185–195.
[18] Ines Álvarez Fernández, Final Engineering Degree Project, University of Oviedo, 2015.
[19] I.I. Cuesta, J.M. Alegre, C. Rodríguez, Mechanical behavior and failure analysis of recycled polymers by use of miniature punch specimens, J. Appl. Polym. Sci. http://dx.doi.org/10.1002/app.42911.
[20] J. Cailloux, R.N. Hakim, O.O. Santana, J. Bou, T. Abt, M. Sánchez-Soto, F. Carrasco,

M.L. Maspoch, Reactive extrusion: a useful process to manufacture structurally modified PLA/o-MMT composites, Compos. Part A: Appl. Sci. Manuf. 88 (2016) 106–115.
[21] M.L. Maspoch, E. Franco-Urquiza, J. Gamez-Perez, O.O. Santana, M. Sánchez- Soto, Fracture behaviour of poly[ethylene–(vinyl alcohol)]/organo-clay composites, Polym. Int. 58 (6) (2009) 648–655.

Table 1
Mean values and standard deviations of tensile and small punch test parameters.

Material	E (GPa)	σ_y (MPa)	ε_y (%)	$Slope_{ini}/t$ (MPa)	P_{ym}/t^2 (MPa)	d_{ym}/t (mm/mm)
PP	2.4 ± 0.1	21 ± 1	3.9 ± 0.1	95 ± 8	200 ± 11	5.3 ± 0.4
PET	3.3 ± 0.1	65 ± 2	2.5 ± 0.1	150 ± 13	497 ± 40	3.7 ± 0.6
PETG	2.8 ± 0.2	58 ± 1	2.6 ± 0.2	125 ± 20	497 ± 23	4.2 ± 0.5
PLA_0%	3.9 ± 0.1	65 ± 1	1.9 ± 0.1	200 ± 17	618 ± 32	4.2 ± 0.8
PLA_0T	3.5 ± 0.2	52 ± 1	2.7 ± 0.1	155 ± 11	453 ± 24	4.8 ± 0.4
PLA_0.5%	3.9 ± 0.3	74 ± 2	2.5 ± 0.2	195 ± 10	620 ± 44	4.6 ± 0.7
PLA_0.5T	3.6 ± 0.2	65 ± 1	2.7 ± 0.4	160 ± 13	487 ± 30	5.2 ± 0.3
PLA_2.5%	4.0 ± 0.1	74 ± 1	2.2 ± 0.2	200 ± 9	604 ± 12	4.5 ± 0.5
PLA_2.5T	3.8 ± 0.1	68 ± 2	2.4 ± 0.2	180 ± 15	529 ± 19	4.9 ± 0.4
EVOH_0%	3.6 ± 0.4	62 ± 2	3.6 ± 0.3	197 ± 10	538 ± 30	6.6 ± 0.9
EVOH_1%	3.6 ± 0.3	53 ± 1	3.6 ± 0.1	151 ± 4	460 ± 35	6.0 ± 0.5
EVOH_2.5%	3.2 ± 0.6	54 ± 1	3.2 ± 0.1	134 ± 8	441 ± 27	6.2 ± 0.8

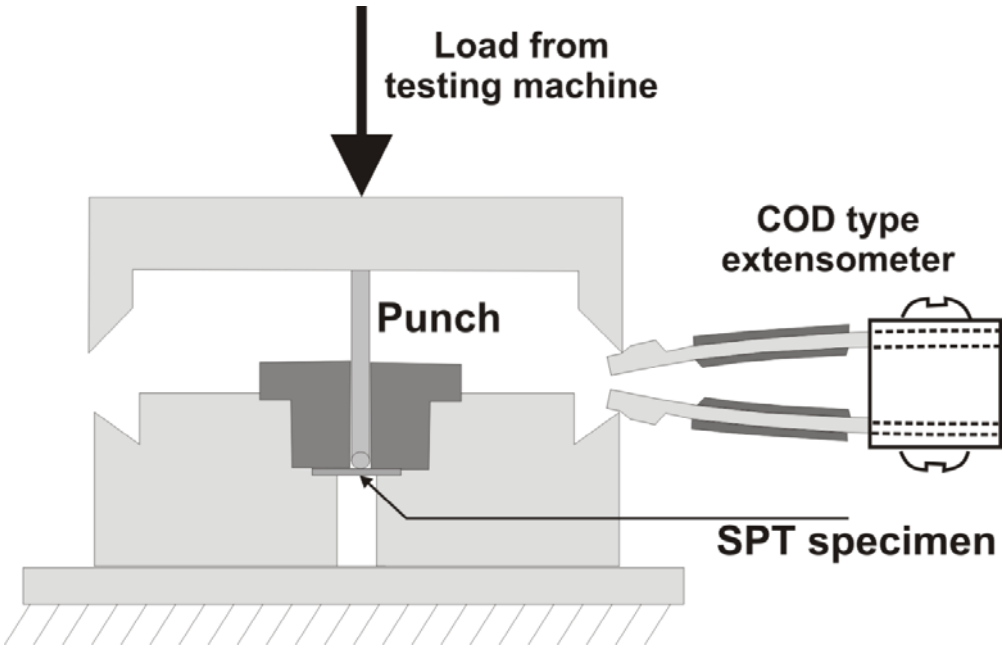

Figure 1. Small punch test configuration

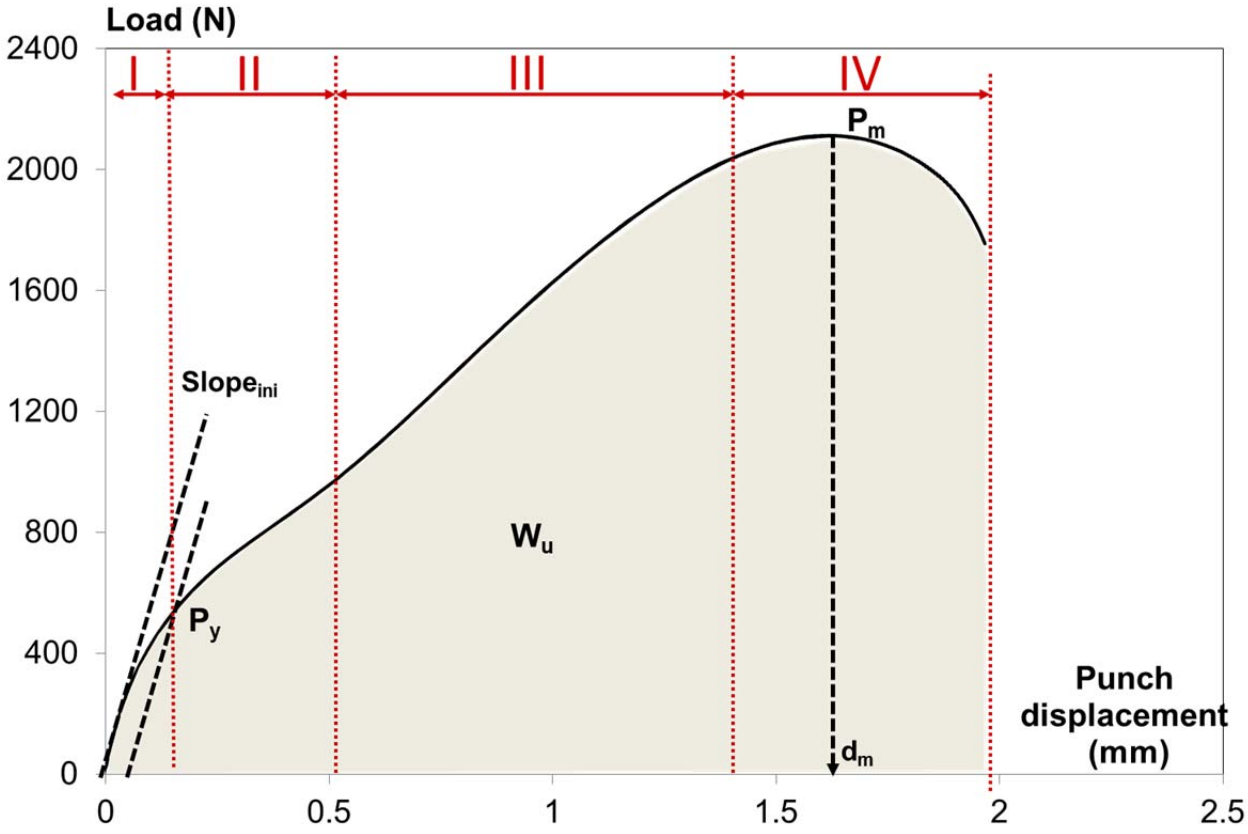

Figure 2. Typical SPT plot obtained with a ductile steel specimen

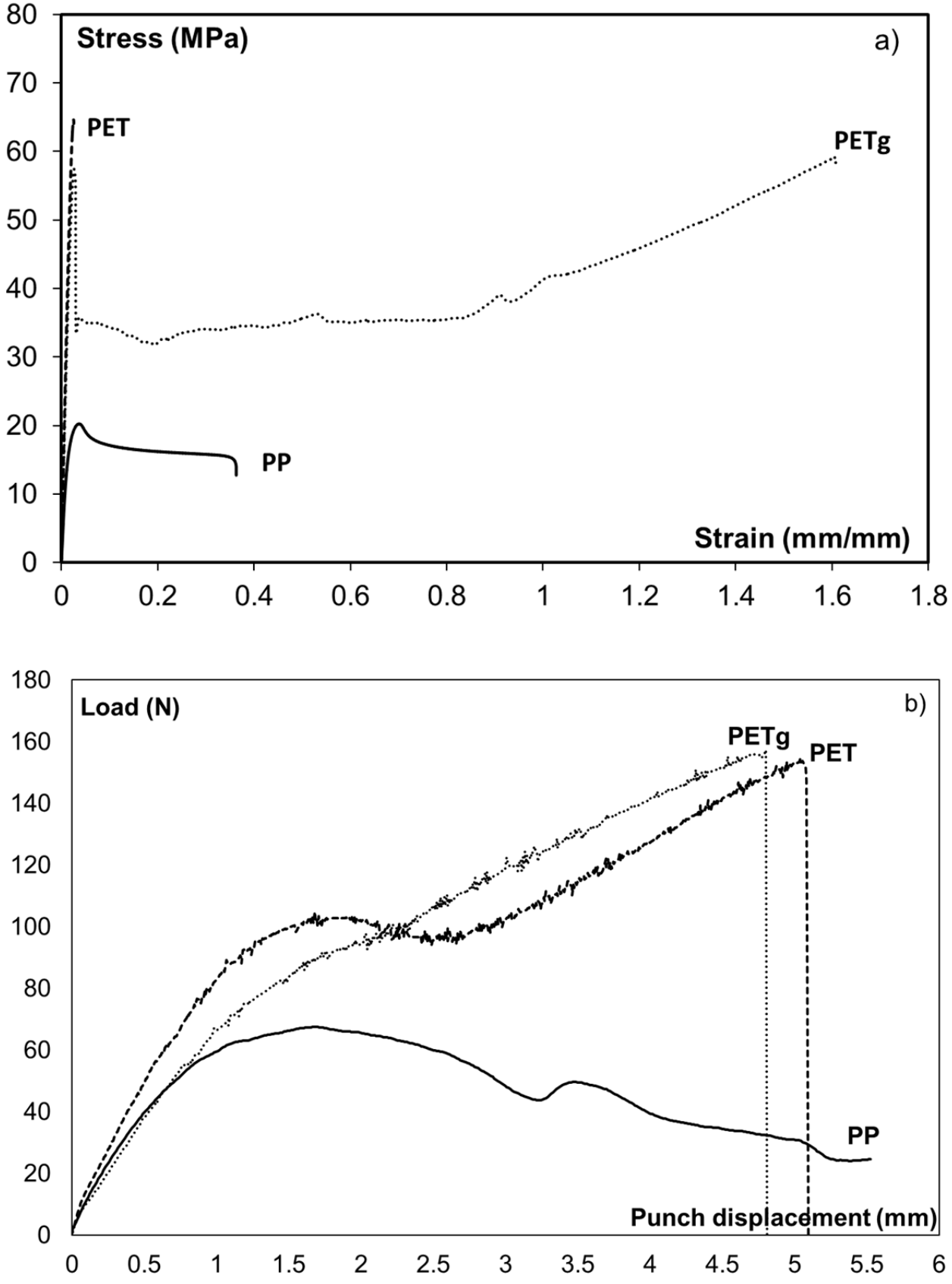

Figure 3. PP [19], PET and PETg characteristic curves from: a)Tensile test (b) SPT

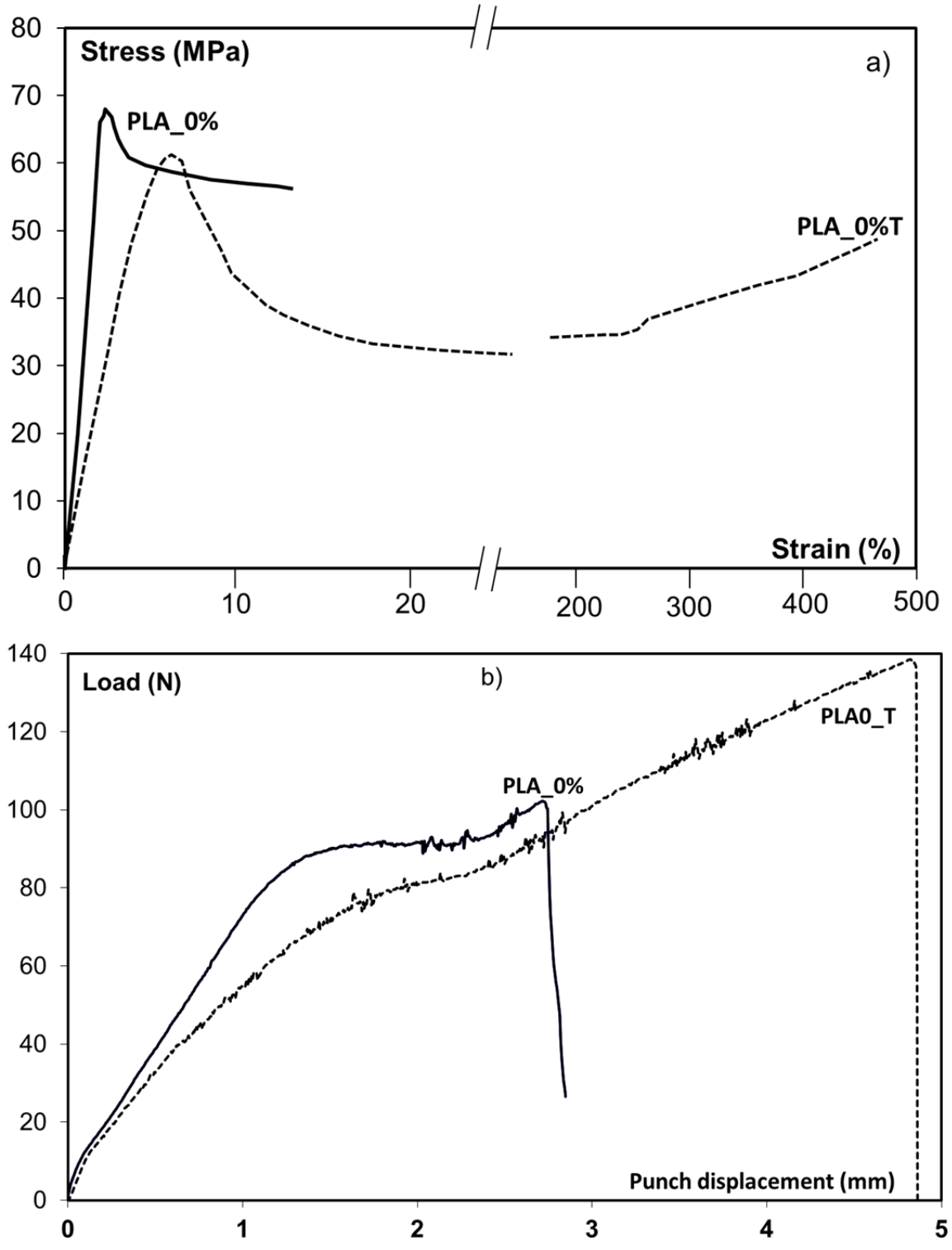

Figure 4. PLA's characteristic curves from: a)Tensile test (b) SPT [16]

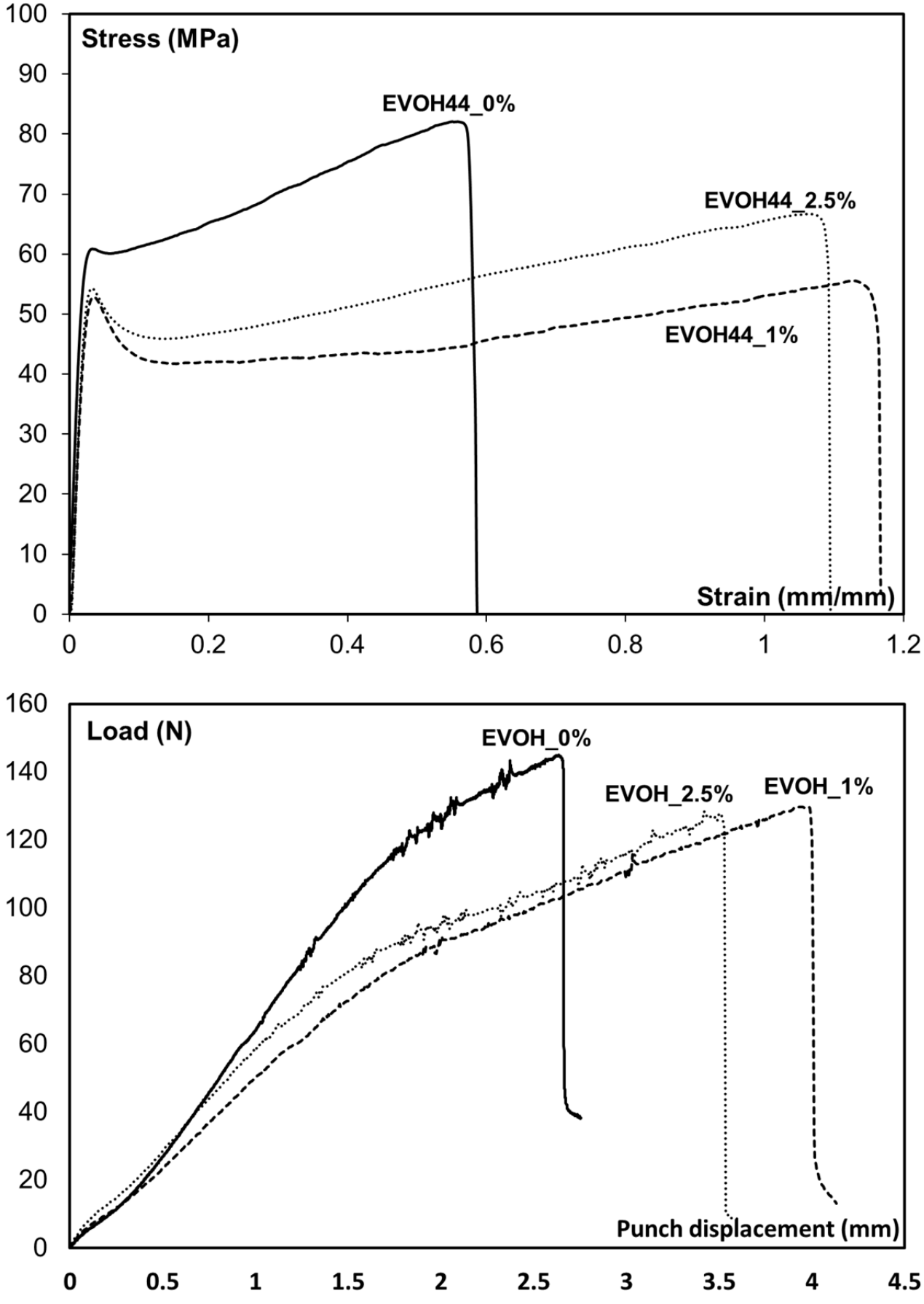

Figure 5. EVOH's characteristic curves from: a)Tensile test (b) SPT

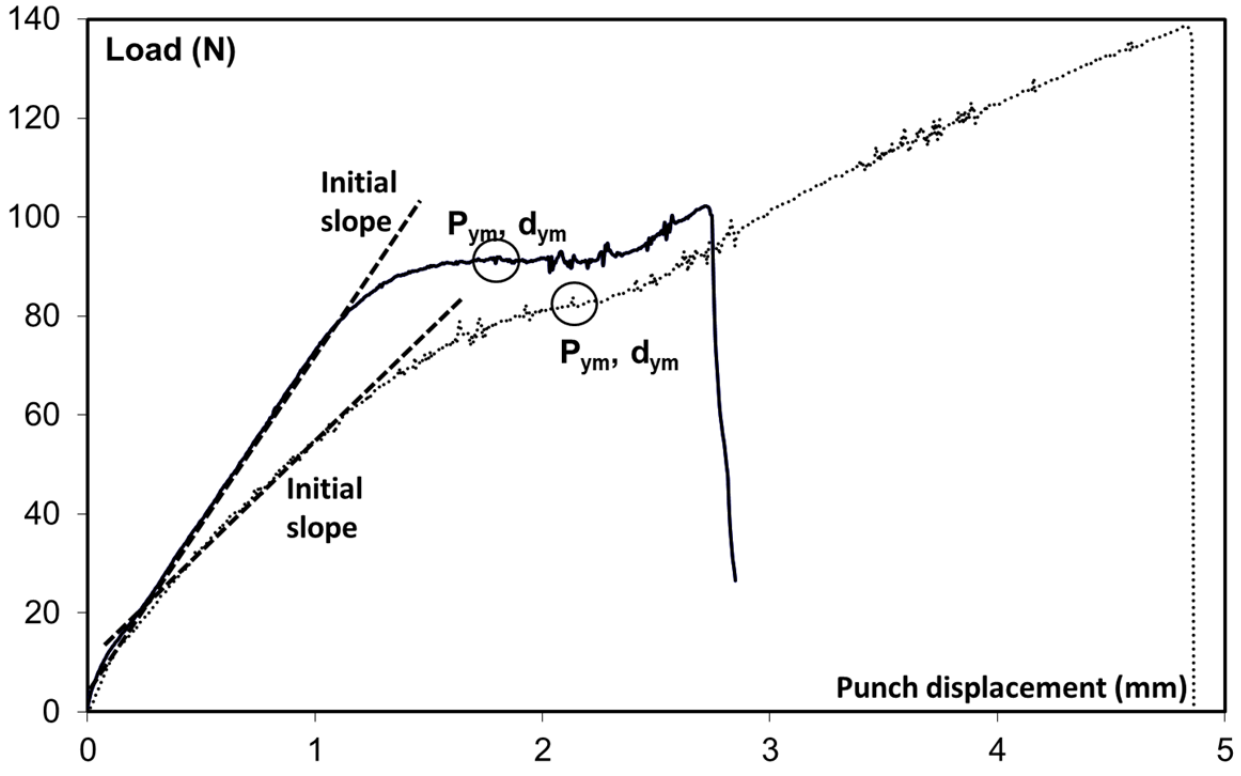

Figure 6. Characteristic points in the load-displacement SPT curves obtained with polymers

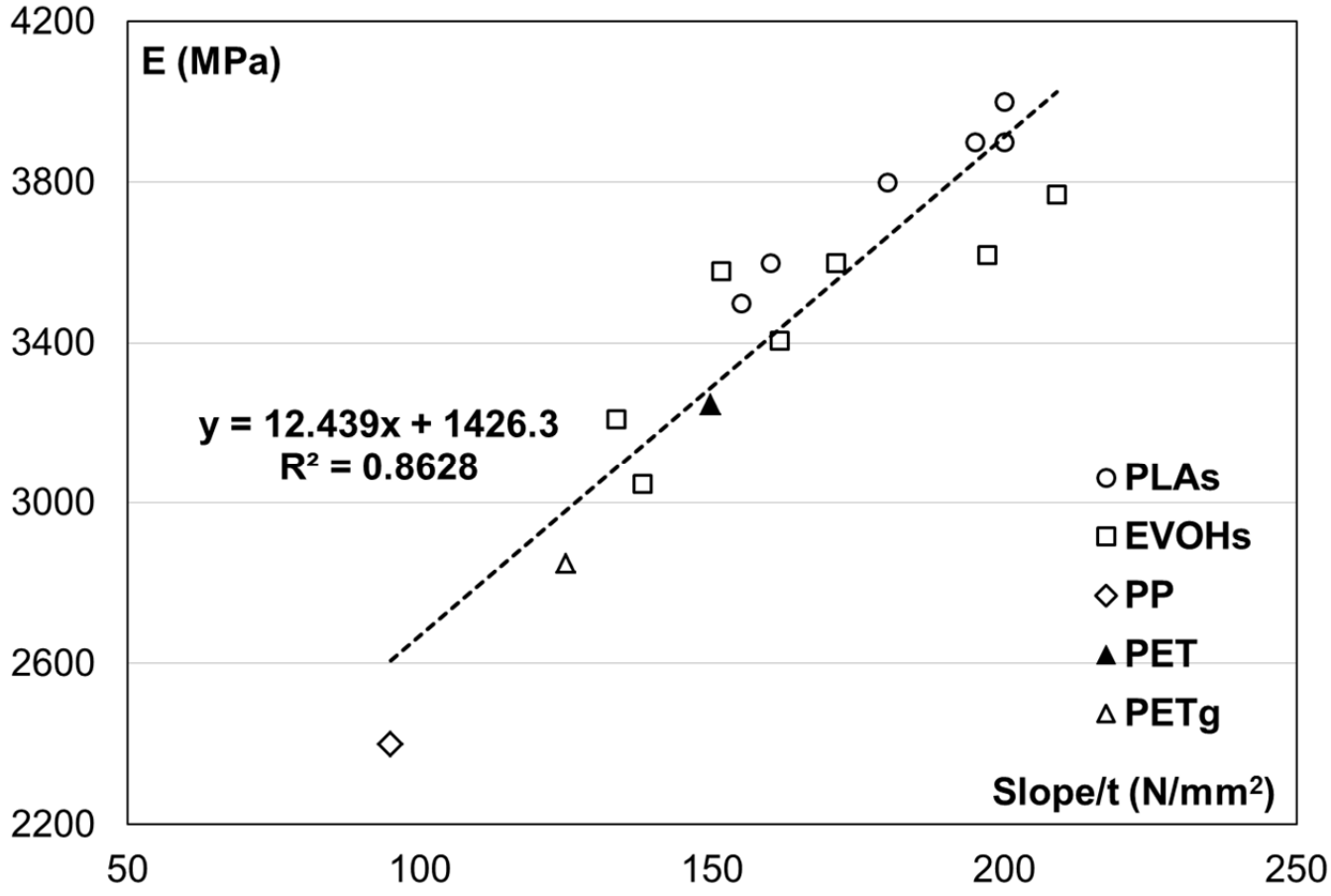

Figure 7. Relationship between the tensile elastic modulus, E, and the Slope/t SPT parameter

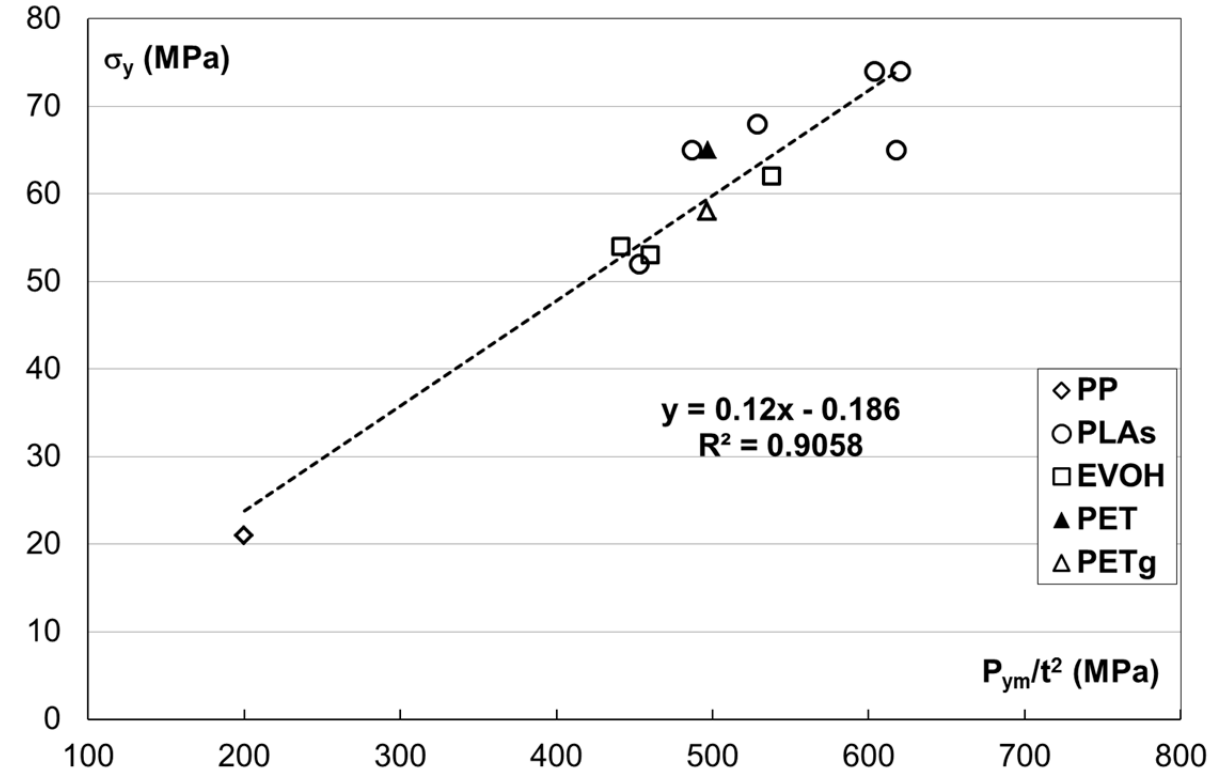

Figure 8. Relationship between the tensile yield strength, σ_y, and the P_{ym}/t^2 SPT parameter

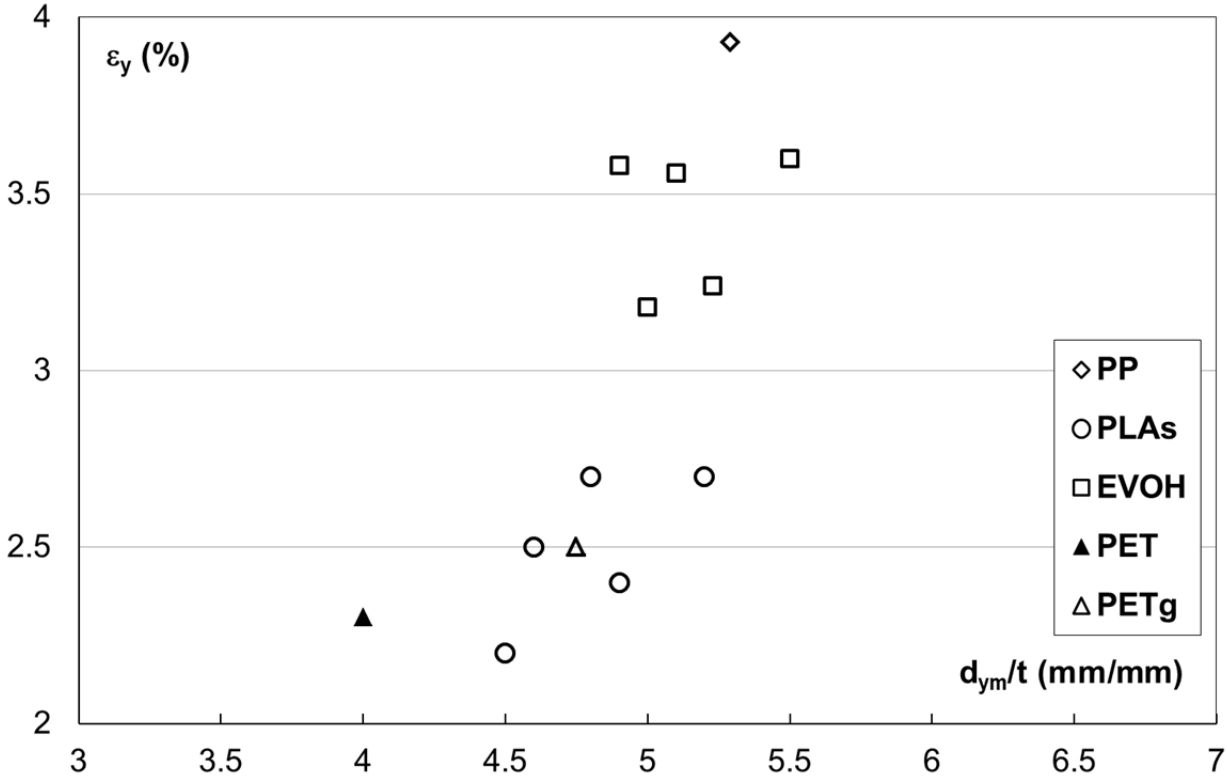

Figure 9. Relationship between the tensile yield strain, ε_y, and the d_{ym}/t SPT parameter